SEE CORRECTION FOR THIS ARTICLE
RESEARCH ARTICLE | NEUROSCIENCE

Microglia phagocytosis mediates the volume and function of the rat sexually dimorphic nucleus of the preoptic area

Lindsay A. Pickett[a,b], Jonathan W. VanRyzin[a,b], Ashley E. Marquardt[a,b], and Margaret M. McCarthy[a,b,1]

Edited by Donald Pfaff, Rockefeller University, New York, NY; received July 22, 2022; accepted January 24, 2023

The sexually dimorphic nucleus of the preoptic area (SDN-POA) is the oldest and most robust sex difference reported in mammalian brain and is singular for its presence across a wide range of species from rodents to ungulates to man. This small collection of Nissl-dense neurons is reliably larger in volume in males. Despite its notoriety and intense interrogation, both the mechanism establishing the sex difference and the functional role of the SDN have remained elusive. Convergent evidence from rodent studies led to the conclusion that testicular androgens aromatized to estrogens are neuroprotective in males and that higher apoptosis (naturally occurring cell death) in females determines their smaller SDN. In several species, including humans, a smaller SDN correlates with a preference for mating with males. We report here that this volume difference is dependent upon a participatory role of phagocytic microglia which engulf more neurons in the female SDN and assure their destruction. Selectively blocking microglia phagocytosis temporarily spared neurons from apoptotic death and increased SDN volume in females without hormone treatment. Increasing the number of neurons in the SDN in neonatal females resulted in loss of preference for male odors in adulthood, an effect paralleled by dampened excitation of SDN neurons as evidenced by reduced immediate early gene (IEG) expression when exposed to male urine. Thus, the mechanism establishing a sex difference in SDN volume includes an essential role for microglia, and SDN function as a regulator of sexual partner preference is confirmed.

sex dimorphism | preoptic area | microglia | phagocytosis | neurodevelopment

Significance

Establishing the origins of brain sex differences is an essential goal for understanding phenotypic variance in behavior. The sexually dimorphic nucleus (SDN) is the oldest known and most robust anatomical sex difference in the mammalian brain. Its origins have long been assumed to be due to differential cell autonomous apoptosis, and the larger SDN correlated with preference for females as sexual partners, but these premises have been unproven. Data generated in rats establish that the mechanism establishing a sex difference in SDN neuron number involves an essential role for microglia as ultimate purveyors of cell death which may begin with the neurons. This early process, not the ultimate size of the SDN, is an arbiter of sexual partner preference in adulthood.

The sexually dimorphic nucleus of the preoptic area (SDN-POA) has been a brain region of intense interest since its discovery in the rat brain in 1978 (1). Named for its primary feature, the SDN-POA was the first macrolevel sex difference reported for the mammalian brain and followed directly from the discovery of large sex differences in the volume of song control nuclei in songbirds (2).

The mammalian POA resides bilateral to the third ventricle and is bordered dorsally by the anterior commissure, ventrally by the optic chiasm, and lies just anterior to the hypothalamus (Fig. 1*A*), sometimes being considered a subdivision therein. It is best known for gating an array of behaviors associated with reproduction in both sexes (3). The medial preoptic nucleus (MPN) resides within the POA and is subdivided into lateral, medial, and central subdivisions. The SDN is largely overlapping with but not exclusive to the central subdivision of the MPN and is sometimes referred to as the MPNc. The volume of the rodent SDN is two to four times larger in males than females and can be revealed with a simple Nissl stain (4). It is also defined by a subset of cells that are immunopositive for Calbindin-D28k (a calcium-binding protein expressed in GABAergic neurons) and thus often referred to as the CALB-SDN (5, 6). Sex differences in the SDN and the CALB-SDN are of the same magnitude, and larger size positively correlates with a preference for mating with females across an array of mammalian organisms from shrews and gerbils to domesticated sheep and humans (7). Male sheep which exhibit a sexual preference for male partners have an intermediate SDN volume when compared to female-oriented rams and to ewes (8). The findings of this ovine study are mirrored by that of two human studies which investigated the size of the interstitial nucleus of the anterior hypothalamus–3 (INAH-3), considered the human homolog of the SDN, in presumed heterosexual and homosexual men and heterosexual females (9, 10); however, these studies did not investigate INAH-3 size in homosexual females and have been subject to critique by scholars who argue the work oversimplifies human sexuality into rigid binary categories and then imposes them onto a "dimorphic" brain structure which is in reality also complex in its size distribution across individuals (11, 12). Regardless, the combination of the SDNs status as the first large neuroanatomical sex difference in the mammalian brain and its potential role in sexual partner preference has made it the topic of intense scrutiny, with an emphasis on two questions: 1) by what mechanism is the sex difference established,

Author affiliations: [a]Department of Pharmacology, University of Maryland School of Medicine, Baltimore, MD 21201; and [b]Program in Neuroscience, University of Maryland School of Medicine, Baltimore, MD 21201

Author contributions: L.A.P., and M.M.M. designed research; L.A.P., J.W.V., A.E.M., and M.M.M. performed research; L.A.P., J.W.V., A.E.M., and M.M.M. analyzed data; and L.A.P., J.W.V., A.E.M., and M.M.M. wrote the paper.

The authors declare no competing interest.

This article is a PNAS Direct Submission.

[1]To whom correspondence may be addressed. Email: mmccarthy@som.umaryland.edu.

This article contains supporting information online at https://www.pnas.org/lookup/suppl/doi:10.1073/pnas.2212646120/-/DCSupplemental.

Published February 27, 2023.

and 2) what is the functional impact of a sex difference in size? To this day, neither question has been definitively answered.

The canonical view of sexual differentiation of the mammalian brain centers on a perinatal critical period beginning with steroidogenesis by the fetal testis. This bathes the developing brain in androgens to exert direct effects via androgen receptors (AR) and, in the case of rodents, frequently via estrogen receptors (ER) following local aromatization of testosterone to estradiol within neurons (13). Direct programming of cellular processes, presumably via AR- and ER-mediated transcription (14–16), is believed to drive the masculinization of the brain away from the female phenotype which occurs in the absence of testicular steroids. The volumetric sex difference of the SDN in rodents is entirely reversible by either exogenous estradiol administration to females or preventing/antagonizing estradiol action in males during the critical period (17).

Attempts to determine how gonadal steroids drive the sex difference in the size of the SDN began in earnest shortly after its discovery and followed the logic that there are three principal means by which this could occur: 1) More neurons are born and incorporated into the male SDN, 2) more neurons migrate into and take up permanent residence in the male SDN, or 3) more neurons die in the female SDN. In rodents, neurogenesis of the SDN begins at embryonic day 14 (E14) and ends after E18 with little to no evidence of sex differences in the number of neurons born (18, 19), eliminating option #1. The cells ultimately making

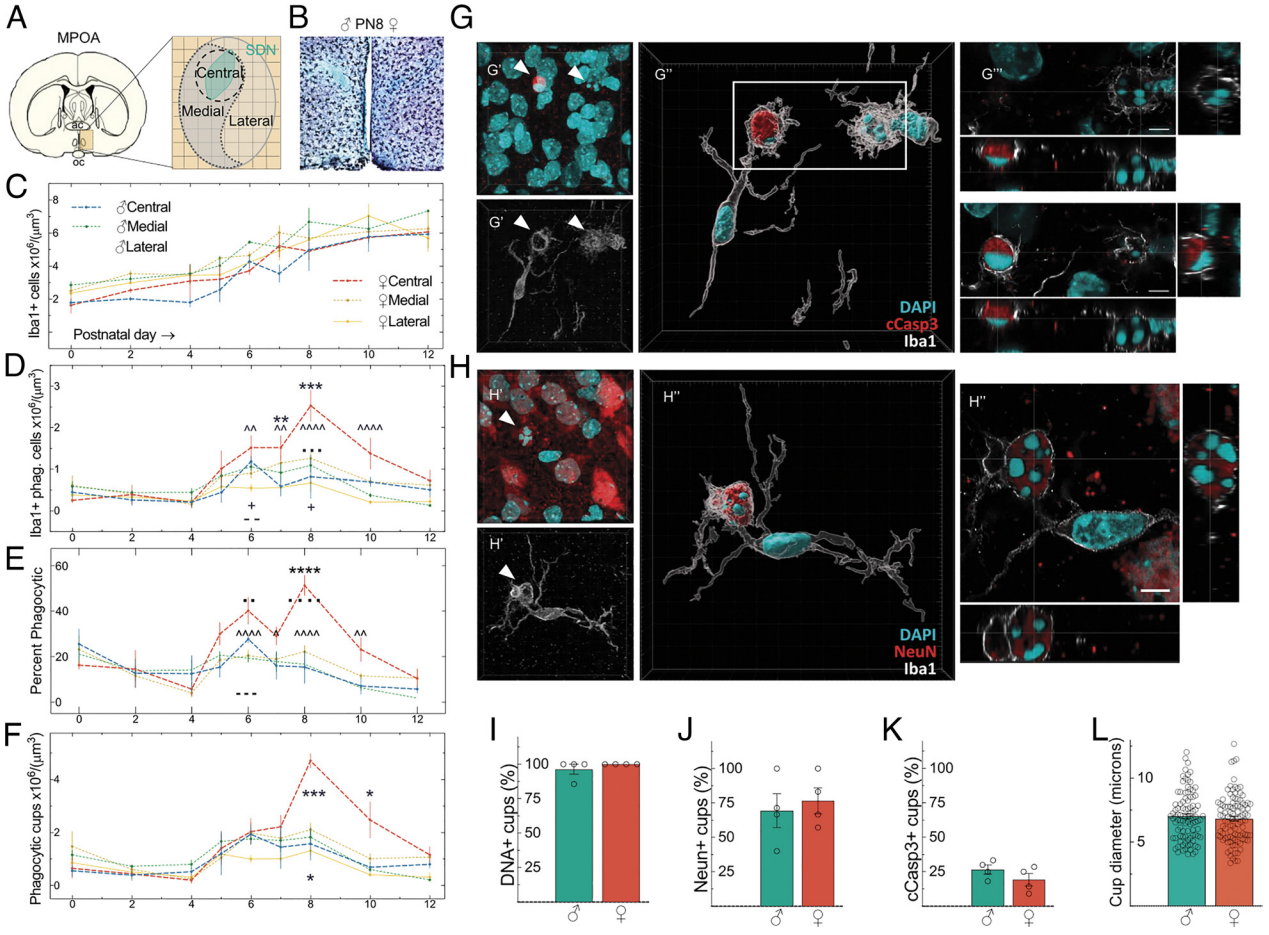

Fig. 1. Neurons of the female SDN are eliminated by microglial phagoptosis. (*A*) Schematic representation of the 100 µm × 100 µm grid used to trace subdivisions of the MPN to count and characterize microglia from day of birth (PN0) to PN12. (*B*) Photomicrograph of Iba1+ microglia in the MPN in both sexes at PN8. Nissl-SDN was visualized with methyl green and used as a guide for grid placement for microglia quantification. (*C*) Iba1+ microglia increasingly populate the medial preoptic nucleus across the first 12 postnatal days with no differences between males and females. A main effect of age [$P < 0.0001$); F(8, 164) = 47.13] and subdivision [$P < 0.0001$; F(8, 164) = 47.13] was detected. Both males and females had the highest number of microglia within the mMPN subregion. Bars represent the mean ± SEM. (*D*) The female central cMPN has a higher density of phagocytic microglia when compared to males on PN7 (**$P = 0.0098$) and PN8 (***$P < 0.001$), as well as when compared to the mMPN on PN8 (···$P = 0.0003$), and lMPN on PN6, (^^$P = 0.0019$), PN7 (^^$P = 0.0023$), and PN8/10 (^^^^$P < 0.0001$). The male cMPN contains a higher density of phagocytic microglia than the mMPN on PN6 (- -$P < 0.01$) and the lMPN on PN6 and 7 (+$P < 0.05$). (*E*) The female central cMPN has a higher percentage of phagocytic microglia when compared to males on PN8 (****$P < 0.0001$) as well as when compared to the medial PN6 (···$P = 0.0014$), PN8, (···$P < 0.0001$) and lateral on PN6/8 (^^^^$P < 0.001$), PN7 (^$P = 0.0112$), and PN10 (^^$P = 0.0023$). Males have a greater percentage of phagocytic microglia in the central vs. lateral MPN on PN6 (- - -$P = 0.001$). (*F*) A main effect of sex was detected in the central [$P = 0.002$; F(1, 52) = 10.35] and lateral [$P = 0.002$, F(1, 43) = 10.88] but not medial mPOA, indicating females had more phagocytic cups than males in those regions. The female central cMPN has a higher density of phagocytic cups when compared to males on PN8 (***$P < 0.001$) and PN10 (*$P = 0.0164$), and within the lMPN subregion, females have a higher number of phagocytic cups than males on PN8 (*$P = 0.014$). (*G*) Maximum intensity projection (MIP) of DAPI (cyan) and cleaved caspase-3 (cCasp3; red), and Iba1 (grey). (*G'*) White arrowheads indicate phagocytic cups. (*G''*) Three-dimensional rendering shows phagocytic microglia engulfment of both cCasp3+ and cCasp3− nuclei. Grid line spacing is 5 µm. White box indicates boundary of *G'''*. Orthogonal views focused through the center of the rightmost cCasp3−/DAPI+ phagocytic cup (*Top*) and the leftmost cCasp3+/DAPI+ phagocytic cup (*Bottom*) highlighting the inclusion of cCasp3 and DAPI within boundaries of the cup. (Scale bars, 4 µm.) (*H*) MIP of DAPI (cyan) and NeuN (red) and Iba1 (grey). (*H'*) White arrowheads indicate phagocytic cups. (*H''*) Three-dimensional rendering shows phagocytic microglia engulfment of NeuN+ nuclei. Grid line spacing is 5 µm. (*H'''*) Orthogonal view of the phagocytic cup demonstrating colocalization of NeuN and DAPI within the cup. (Scale bar, 4 µm.) (*I*) Close to 100% of phagocytic cups contained DNA in males and females. (*J*) The majority of the microglial cups surveyed were DAPI+ and Neun+ indicating microglia primarily engulf neuronal cell bodies. (*K*) Less than 25% of neurons detected were positive for cCasp3, a cell death marker. (*L*) Measurement of phagocytic cup diameter cMPN from four PN8 animals (~10 cups/animal) yielded no sex differences and an average diameter of 7 µm.

up the SDN are born in the ventral MPOA, and birth-dating and tracking find no sex difference in that process (19), eliminating option #2. The sensitive period, the time during which the size of the SDN is influenced by gonadal steroids, is from E18 to postnatal day 4 (PN4) (17, 20), but the sex difference does not begin to arise until later, when higher numbers of cells undergoing apoptotic cell death, as evidenced by nuclei exhibiting DNA fragmentation, are observed in females between PN6-9 (21, 22). Consistent with the role of apoptosis as the purveyor of sexual differentiation of the SDN, the rodent male SDN has higher expression of antiapoptotic Bcl-2, while the female SDN exhibits higher expression of pro-apoptotic Bax during the time that the sex difference emerges. Apoptosis via caspase-3 activation occurs at higher rates in the rodent female SDN, and this corresponds with the smaller size of the female SDN (23). Moreover, the sex differences in proapoptotic Bax and Bcl-2 are abolished in response to the treatment of females with a masculinizing dose of estradiol (24, 25), and blocking the translation of ER-alpha within SDN neurons by antisense oligonucleotides prevents masculinization (26).

This combination of observations from multiple independent laboratories led to the irrefutable conclusion that locally aromatized estrogens derived from testicular androgens in fetal males promotes the survival of SDN neurons, at least in rodent species. Female SDN neurons, lacking the putative survival factor provided by estrogens, were thought to succumb to naturally occurring apoptotic cell death, thereby generating the sex difference. By what means estradiol promotes higher survival has eluded discovery. Intriguingly, when the sex difference in the size of the CALB-SDN was investigated in a Bax knockout mouse, there was no significant increase in the size of the CALB-SDN in females as compared to wild type counterparts, whereas the sex difference in the volume of the neighboring BNSTp was abolished by Bax deletion (27). This puzzling observation has been left unexplained, but it suggests that entirely cell autonomous apoptotic cell death is not the only source of the sex difference in SDN volume. Nonetheless, the conclusion that cell autonomous apoptotic cell death is the sole basis for the sex difference in volume of specific brain regions or nuclei has been entrenched in the literature for over 30 y and has formed the basis for similar conclusions for multiple other brain regions that vary in size between males and females (28).

More recent mechanistic studies on the origins of sex differences in the brain have revealed a surprisingly diverse array of region-specific cellular processes, establishing parameters ranging from synaptic density profiles, to dendritic morphology, to control of astrocyte and neuron number (29). Even more surprising has been the central role for inflammatory signaling molecules and immune cells in the establishment of neuroanatomical features which undergird behavioral and physiological sex differences in adolescence and adulthood (30). Of interest here are microglia, the resident immune cells of the brain, which are essential partners in sculpting neural circuits as they develop (31). As modified macrophages, microglia are highly phagocytic and capable of pruning away unnecessary or underutilized synapses (32), as well as engulfing and removing debris following cell death or injury (33). More recently, rather than removing dead cells, microglia have been found to engage in primary phagocytosis, or the active engulfment of a living cell and subsequent induction of its death. This is a common process carried out by peripheral macrophages but has only been discovered in the CNS in the past decade (34), and has since been named phagoptosis for its distinct role in removal of living cells that are viable and would otherwise survive if not actively engulfed and destroyed by microglia (35). Cells targeted for phagoptosis are often distressed due to a subtoxic insult or physiological activation by other means (36). In these instances the apoptosis program is initiated within the cell, i.e., cell autonomous, and simultaneously the dying cell releases "find me" signals and/or displays "eat me" signals that attract phagocytes (37) which then complete the death process via an oxidative burst (38, 39) or other means (40). However, in select regions of the developing brain, these cells are healthy precursors targeted by phagoptosis as a means for regulating population density (41, 42).

We report here a higher rate of microglia-mediated phagoptosis of mature neurons in the SDN of developing female rats, resulting in fewer neurons and a smaller SDN volume and which, when prevented, temporarily results in neuron survival in females and a larger SDN. We further report that this enduringly impacts the preference for male odor in adulthood, thereby definitively establishing both the origins and the function of this small subnucleus within the mammalian preoptic area.

Results

Sex Differences in Microglial Phagocytosis in the MPN. Coronal brain sections were processed through the MPN (Fig. 1*A*) from rat pups ranging in age from day of birth to 12-d-old and microglia visualized by immunohistochemistry for the cell specific marker Iba1 (allograft inflammatory factor 1). Sections were counterstained for Nissl with Methyl Green (Fig. 1*B*), and the boundaries of the medial, lateral, and central subdivisions of the MPN identified based on established histology. Iba1+ microglia increasingly populate the MPN across the first 12 postnatal days (Fig. 1*C*) with no difference in total numbers of microglia between males and females. Both males and females had the highest number of microglia within the medial subregion compared to the central or lateral regions (Fig. 1*C*). The density of microglia with a clearly identifiable phagocytic cup differed by region and sex. In the MPNc females had a higher density of phagocytic microglia compared to males on PN7 and PN8 (Fig. 1*D*) and a greater percentage of microglia were phagocytic in females on PN8 (Fig. 1*E*). Independent of the number of phagocytic microglia, there were more phagocytic cups in the central and lateral subdivisions of the MPN in females. Triple fluorescent confocal images of a phagocytic microglia with activated caspase-3 or the mature neuronal marker NeuN detected inside the phagocytic cup are presented in Fig. 1 *G* and *H*. Combined Iba1 immunohistochemistry and DAPI staining confirmed the presence of DNA in close to 100% of phagocytic cups (Fig. 1*I*), with close to 75% of them also co-staining for NeuN (Fig. 1*J*), while 25% or less costained for the apoptotic marker cCasp3 (activated caspase-3; Fig. 1*K*). The average phagocytic cup diameter was ~7 μM and varied between 3 and 12 μM (Fig. 1*L*). There were no sex differences in any of the above parameters.

Phagocytic Microglia Engulf Viable Neurons of the SDN. In order to determine whether the neurons being engulfed by microglia would otherwise survive, we used three approaches: 1) treatment with the microglia inhibitor minocycline, 2) use of a function-blocking antibody against the CD11b component of complement receptor 3 (CR3) to prevent phagocytosis by disrupting the ability of the microglia to detect and respond to surface complement, commonly considered an eat me signal (43), and 3) use of an additional function-blocking antibody to F4/80, a marker of activated macrophages (44, 45). Treatment of females with minocycline for 3 d (*SI Appendix*, Fig. S2*A*) reduced the number of phagocytic microglia on PN8 (*SI Appendix*, Fig. S2 *B–D*) and induced an intermediate SDN volume in the same animals (*SI Appendix*, Fig. S2*E*). The function-blocking antibodies anti-CR3 and anti-F4/80 were administered directly into the

brain each day from PN5-7, just prior to the peak in microglial phagocytosis on PN8 (Fig. 2*A*). The specific binding of anti-CR3 to microglia was confirmed by immunohistochemistry and found to be widespread (*SI Appendix*, Fig. S2*B*). On PN8 sections were processed for visualization of microglia as above and both SDN volume and cell number quantified (Fig. 2*B*). The higher density of phagocytic microglia and higher number of phagocytic cups in 8-d-old females compared to males was confirmed (Fig. 2 *C* and *D*). Treatment with the function-blocking antibodies significantly reduced the density of phagocytic microglia and phagocytic cups in females. There was no effect of either antibody on the already low percentage of phagocytic microglia in males (Fig. 2 *C* and *D*). Effects were specific to MPNc, as no changes were observed in the lateral subdivision of the MPN in either sex (*SI Appendix*, Fig. S2 *D* and *F*). The volume of the SDN was significantly increased in females treated with anti-CR3 but not anti-F4/80 compared to vehicle-treated females, with no impact of antibody treatment on male SDN volume (Fig. 2*E*). We next sought to confirm that blocking microglia phagocytosis increased the number of neurons that survive in the female SDN. When counted 1 d after the last antibody infusion, on PN8, the number of neurons was significantly higher in control males compared to females but was increased in females treated with either anti-CR3 or anti-F4/80 to the level seen in males. There was no effect of blocking antibody treatment on cell number in male SDN (Fig. 2*F*).

Neonatal Blockade of Microglial Phagocytosis Occludes Female Rat Preference for Male Odors in Adulthood. The ability to increase the volume of the SDN in females without hormone treatment provided a unique opportunity to test the hypothesis that the function of this sexually dimorphic nucleus is to promote a preference for mating with the opposite sex: The notion being that the smaller SDN typical of females promotes a sexual preference for males, while a larger SDN promotes a preference for females. During the normal course of sexual differentiation, testosterone from the fetal testis masculinizes both the appetitive (courtship, odor preference) and consummatory (mounting, intromitting, and ejaculating) components of mating. Thus, one steroid exerts

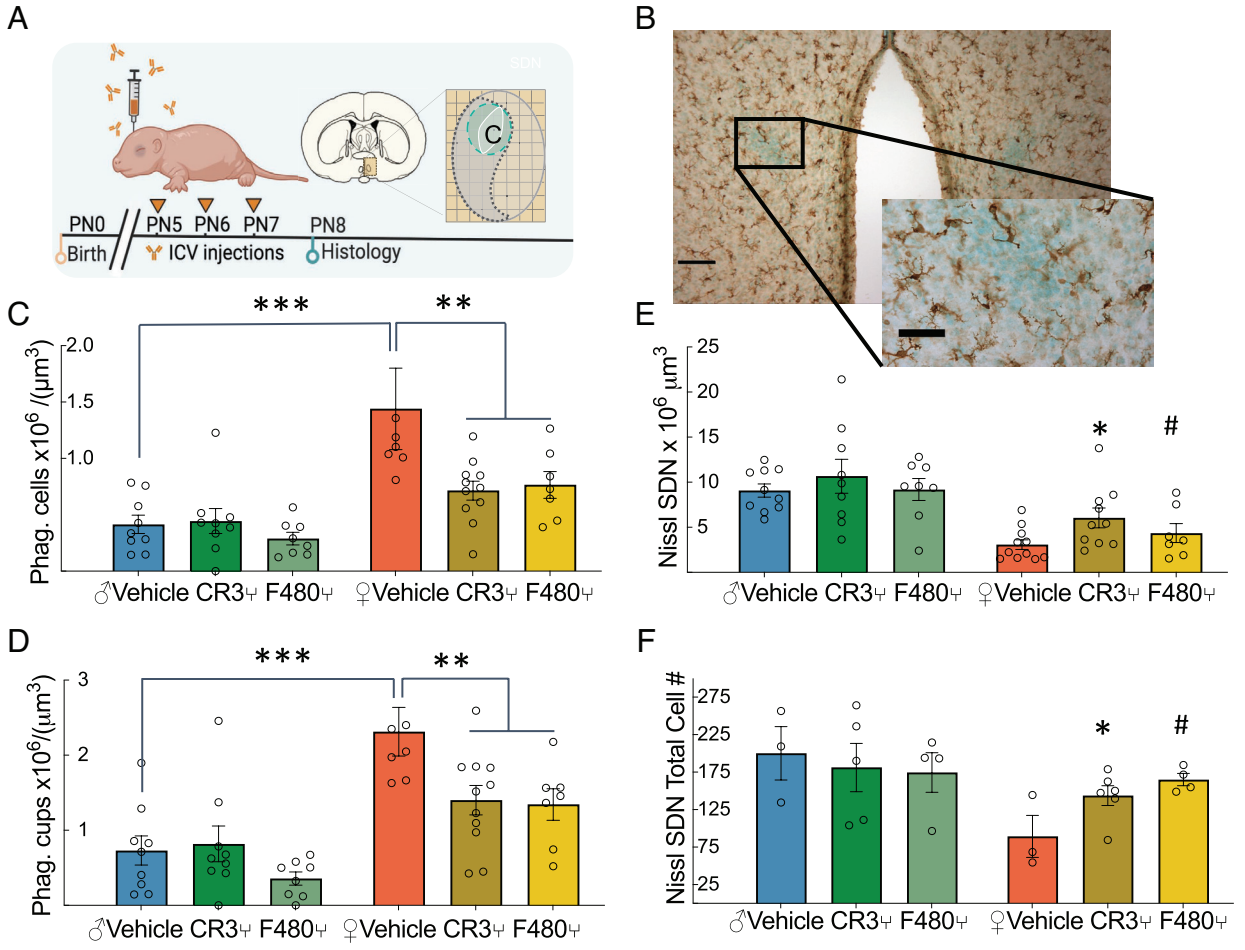

Fig. 2. Antibody-mediated blockade of microglial phagocytosis acutely spares neurons of the female SDN. (*A*) Neonatal pups received bilateral i.c.v. injections of function blocking anti-CR3 and anti-F4/80 antibody on PN5-7. (*B*) Measurements taken on PN8 from coronal sections in which microglia were visualized by immunohistochemistry for Iba1 and SDN cell number and volume determined by Nissl stain taken at 10× (scale bar, 100 µm) and *Inset* at 40× (scale bar, 50 µm). (*C*) A main effect of sex [F(1, 45) = 23.22; ($P < 0.0001$)], treatment [F(2, 45) = 4.049; ($P = 0.0242$)] and interaction of sex and treatment [F(2, 45) = 3.466; ($P = 0.0398$)] was detected for number of phagocytic microglia in the cMPN. Number of phagocytic microglia was greater in female vs. male vehicle groups (***$P = 0.0003$) and was reduced significantly by anti-CR3 (**$P = 0.0023$) or F4/80 antibody treatment (**$P = 0.011$). Bars represent the mean ± SEM for this and all other histograms. (*D*) A main effect of sex [F(1, 45) = 35.07; ($P < 0.0001$)] and treatment [F(2, 45) = 4.52; ($P = 0.016$)] was also detected for number of phagocytic cups. The higher number of phagocytic cups in the female vehicle group compared to males (***$P = 0.001$ was significantly reduced in the female cMPN by anti-CR3 (**$P = 0.0126$) or anti-F4/80 antibody treatment (**$P = 0.017$). (*E*) The male SDN was overall larger than females in all groups [F(1, 45) = 30.75; ($P < 0.0001$)]. Anti-CR3 antibody blockade significantly increased SDN volume in PN8 females (*$P = 0.0325$) while anti-F4/80 trended toward an increase ($^{\#}P = 0.581$; K-W test) compared to vehicle injected females. (*F*) Consistent with the larger volume, there were more cells present in the SDN of all males compared to females [F(1, 19) = 6.51; ($P = 0.196$)]. Post hoc analysis indicated a significant increase in anti-F4/80-treated females ($^{\#}P = 0.03$) and a trend in anti-CR3 antibody-treated females (*$P = 0.08$) compared to vehicle-treated females (Tukey's HSD).

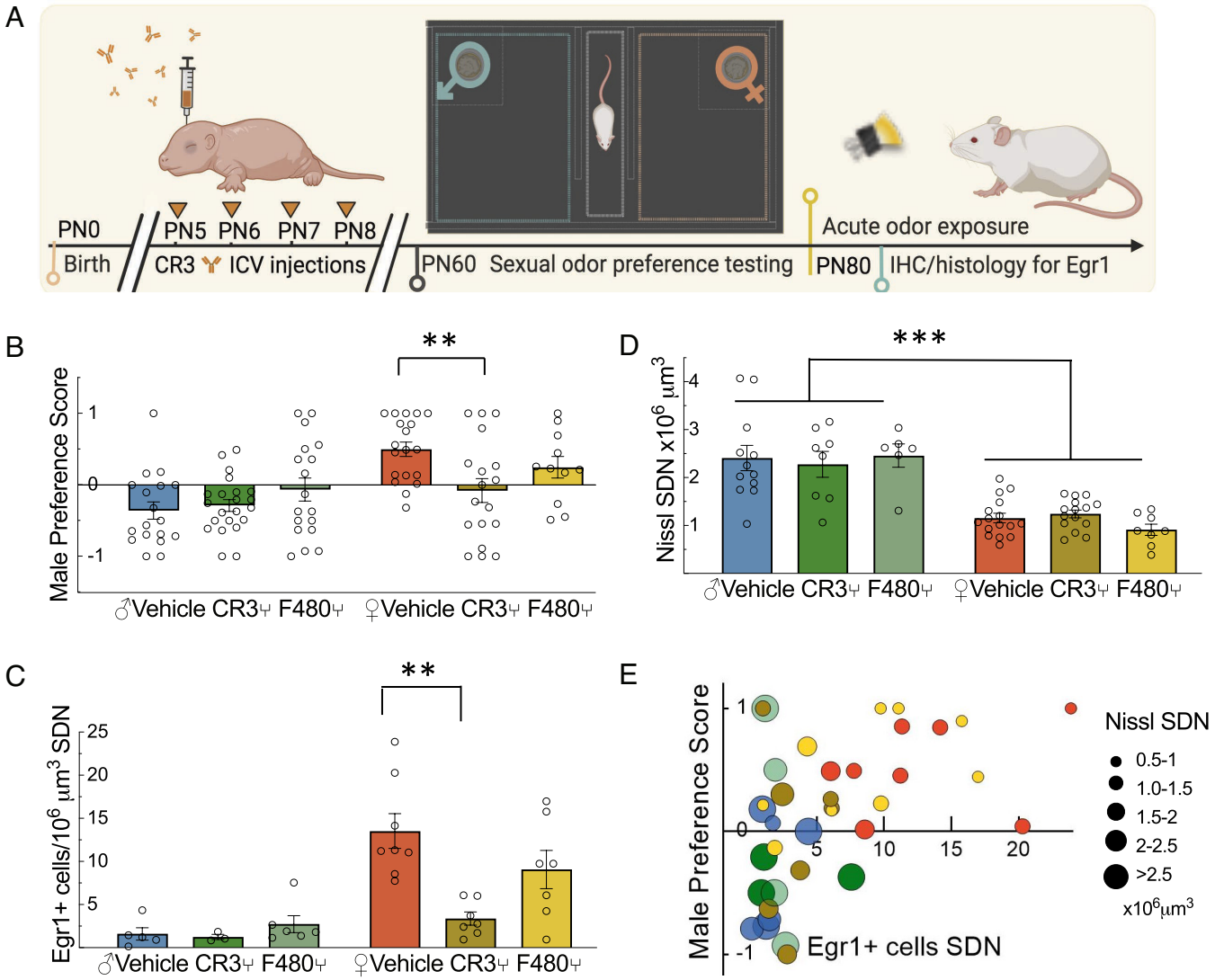

Fig. 3. Neonatal antibody blockade of microglial phagocytosis reduces early growth response protein 1 (Egr1) expression in the cMPN in response to sexually active male odor and sexual partner preference for males in adulthood. (*A*) Neonatal (PN5-8) pups received bilateral i.c.v. injections of vehicle, function-blocking anti-CR3, or anti-F4/80 antibody, and their sexual odor preferences were tested in adulthood (PN60-PN80). On PN80, animals in isolation were acutely exposed to male urine prior to immunohistochemistry for Egr1 expression in the cMPN. (*B*) A male preference score (MPS) was calculated as: MPS = (time in male) − (time in female)/(time in male + time in female) as assessed in a three-chamber apparatus, using soiled bedding from a sexually active male or proestrus female as stimuli, for 5 min following placement of the subject in a neutral (central) zone. A main effect of sex [$F(1, 100) = 17.68$, $P < 0.001$], and an interaction between sex and treatment [$F(2, 100) = 3.75$, $P = 0.0269$] were detected by two-way ANOVA followed by Tukey's multiple comparisons which determined that anti-CR3 antibody-treated females had a significantly reduced MPS compared to vehicle-treated females (**$P = 0.021$). Anti-F4/80 antibody-treated females had an intermediate MPS that was not significantly different from female or male controls. Bars represent the mean ± SEM for this and all other histograms. (*C*) A main effect of sex in number of Egr1+ cells in cMPN was detected by two-way ANOVA [$F(1, 15) = 35.39$, $P < 0.0001$]. Anti-CR3 but not F4/80 antibody-injected animals had significantly reduced numbers of Egr1+ cells in the cMPN following acute male urine odor exposure compared to vehicle females (***$P < 0.001$). (*D*) The Nissl SDN volume was significantly larger in all male treatment groups compared to females on PN80 [$F(3, 31) = 10.82$; ***$P < 0.0001$]. (*E*) A positive correlation was found between the number of Egr1+ cells per unit area in response to acute male odor stimulus and male preference score (Pearson $r = 0.48$ $R^2 = 0.23$; $P = 0.02$). Open circles represent individual data points for each animal and circle size reflects SDN volume.

multiple effects, precluding the ability to isolate the role of the SDN in specific aspects of mating behavior via hormonal manipulation alone. Our discovery of the mechanism establishing the sex difference in SDN size allows a means for teasing out its function away from the overall process of masculinization, but precludes the ability to test whether females with a larger SDN prefer to mate with females, because the neural circuit of mating behavior remains feminized in the absence of neonatal testosterone. Therefore, we used odor preferences as a well-established proxy for sexual preference in rodents (46). Animals were treated in the same manner as above, with anti-CR3 and anti-F4/80 antibodies from PN5-8, but were then raised to adulthood (PN60-80) and tested for sexual odor preference (females during proestrus) using a three-chamber apparatus containing a neutral zone flanked by two choice chambers containing soiled bedding from a sexually active male on one side vs. that of a proestrus female on the other (Fig. 3*A*). Time spent in the choice chambers over a 5-min test was used to calculate a male preference score (MPS). As expected, control males preferred female odors and control females preferred male odors (Fig. 3*B*). However, females treated with anti-CR3 as neonates no longer showed a preference for male odor. Females treated with anti-F4/80 were intermediate in their MPS but were not significantly different from control females.

As reviewed above, prior studies have correlated larger SDN volume with a preference for mating with or for the odors of females, in adults. To confirm this, we counted the number of

neurons and measured SDN volume in the adult animals that participated in the odor preference trial and found, to our surprise, that the number of neurons and the overall size of the SDN of females was smaller than that of males in all treatment groups and independent of odor preference (Fig. 3 *D* and *E*). There was a small but significant increase in the number of neurons in the SDN of anti-CR3-treated females compared to control females, despite there being no difference in volume between the two groups (*SI Appendix*, Fig. S3). These results suggest that neurons of anti-CR3-treated females were more densely packed compared to control females, but both numbers of cells and volume of the SDN were still significantly less than observed in males. We therefore asked whether the activation of neurons within the MPNc in response to opposite sex odors was affected by the neonatal blockade of microglia phagoptosis. To this end, animals were acutely exposed to male odor for 10 min and euthanized within 1 h and assessed for expression of the immediate early gene Egr1 by immunohistochemistry. We first confirmed in naïve animals (uninjected) what has been seen by others (47), that significantly more neurons are activated in the MPNc in response to male odor in females than males, and this was also true in animals receiving vehicle injection (Fig. 3*C*). However, females treated with anti-CR3 as neonates had significantly fewer neurons expressing Egr1 compared to vehicle-injected controls when exposed to male odor as adults and were on par with the low level of activation seen in males (Fig. 3*C*). As with MPS, females injected with anti-F4/80 were intermediate in Erg1+ response and therefore not significantly different from either males or females. That the loss of preference for male odor is independent of the size of the SDN, but negatively correlated with greater numbers of Egr1-expressing neurons, is illustrated in Fig. 3*E*. These data are consistent with the interpretation that the responsiveness of SDN neurons to opposite sex odors is programmed developmentally and that microglia-mediated phagoptosis is not random, but rather selective and necessary for the removal of neurons that are not responsive to male odor in females. How this selectivity is achieved is unknown but is likely to begin with developmental programming of neurons by estradiol in males. When phagoptosis of superfluous SDN neurons in females is disrupted during development, their survival does not increase the volume of the entire nucleus in adulthood but instead results in a more densely packed SDN that is less responsive to male odor cues and required for a female-typical preference for male odors during proestrus.

Discussion

From the time of its discovery, the function of the SDN was presumed to be sex-specific, but determining what that function is has been challenged by its small size, location within the larger MPN, and the fact that its formation is regulated by the same steroid hormones that differentiate many other neuroanatomical and neurochemical endpoints driving differences in reproductive behavior (48). Lesioning the SDN does not interfere with the consummatory components of male mating behavior (49), but, as noted above, the larger size of the SDN and its human homolog correlates with a preference for mating with females, while a smaller SDN parallels a preference for mating with males (7). Although the SDN is a small subnucleus, it is nonetheless highly complex. The MPNc, in which the SDN largely resides, consists mostly of GABAergic inhibitory neurons which also express calbindin, and sometimes corticotrophin releasing factor (CRF), dopamine beta-hydroxylase, and neuropeptide Y (NPY). It also contains cell bodies expressing thyrotropin releasing hormone (TRH) and both fibers and cell bodies containing cholecystokinin (CCK) and somatostatin (50–52). Many of these neuropeptides and neurotransmitters have been implicated in detection of odors of various sorts (53, 54). The ability of neurons in the SDN to selectively respond to odors of the opposite sex has been established and is determined by early life programming via exposure to testosterone and its metabolite estradiol (47), but precisely how the SDN is formed differentially in males and females has been unknown.

Apoptosis is most commonly a cell autonomous event in which a cell participates in its own demise, often due to the lack of some essential process. In the case of the SDN, it was long assumed the process was programmed by developmental exposure to estradiol. Moreover, the long delay between the timing of steroid exposure and the appearance of the sex difference in SDN volume seemed consistent with the notion of a developmental process, such as synaptic wiring, that takes time and if not successfully completed would lead to initiation of a cell death program. Taking this a step further, Forger and colleagues speculated the genes coding for the essential process were epigenetically suppressed by DNA methylation in females, a notion supported by the observation that treatment of newborn female mice with the DNA methylation inhibitor zebularine increased neuronal survival in the SDN (55), but by what means was unknown. More recently, Roselli and colleagues characterized the epigenetic landscape of the domestic ram hypothalamus, which contains the ovine SDN, and compared males that reliably and enduringly prefer to mate with other rams with those that prefer ewes, finding large numbers of differentially expressed genes (56). We now report that rather than solely cell-autonomous apoptosis determining the sex difference in SDN volume, phagocytosis of neurons by microglia in females reduces the size of the SDN. The treatment of females with an anti-CR3 antibody which masks the putative eat me signal identified by microglia, or a blocking antibody to F4/80 which is associated with activated microglia, allows the neurons to survive, temporarily increasing neuron number and resulting in a larger SDN. The impact of the anti-CR3 antibody was the greatest, implicating the complement system as the major mediator of this differential phagoptosis, as has been shown in other systems, including regulation of a sex difference in astrocyte populations in the medial amygdala (41). That the cellular targets in the SDN were mature neurons was confirmed by the detection of the neuronal marker NeuN in the majority of phagocytic cups. In other systems, the process of apoptosis begins in a cell and this attracts phagocytes which complete the death process in an "assisted suicide" (38, 39). We detected activated caspase-3 in only 25% of phagocytic cups but cannot rule out the potential for other apoptotic mediators or the expression of find me and/or eat me and "don't eat me" signals in SDN neurons that are determined by estradiol exposure. Microglia are highly responsive to the environment in which they find themselves (57) and thus are likely responding to signals emanating from the neurons.

We confirmed that reduced microglia phagoptosis in females increased the number of neurons and produced a larger SDN when assessed shortly after antibody infusion. The effectiveness of blocking antibodies is expected for only as long as the antibodies are available, and this proved true when the volume of the SDN was assessed 2 mo after the last antibody infusion and found to be in the typical female range. The canonical view has been that volumetric sex differences such as that involving the SDN are established during perinatal sexual differentiation and then passively maintained throughout life. This was reframed with the discovery that new cells are continuously added to the SDN, as well as two other sexually dimorphic nuclei, the anteroperiventricular nucleus (AVPV) which is larger in females, and the medial amygdala which is larger in males (58). Phenotyping of the adult-added cells revealed mostly neurons (neuronal nuclei - NeuN+)

in the AVPV and a mix of neurons and astrocytes (glial fibrillary acidic protein - GFAP+) in the medial amygdala, but the newly added cells of the SDN were unidentifiable (58). We found that adult females in which microglia-mediated phagocytosis within the SDN was temporarily blunted during its normal developmental peak behaviorally lost the preference for male odor; additionally, these females exhibited little signs of neuronal activation within the SDN following acute exposure to male odor as compared to control females which exhibited a robust activation to male odor. The known epigenetic regulation of SDN volume (55) combined with our current data suggests a complex interplay of early life programming of SDN cells to be activated by opposite sex odors in adulthood, which tags specific cells and/or precursors for elimination if that criteria is not met. Moreover, our findings demonstrate it is not the size of the SDN that matters in adulthood, but rather the sensitivity of the neurons to opposite sex odor. Thus, the larger SDN normally found in males may be a byproduct of reduced phagoptosis of cells within the nucleus, instead of being causally related to partner preference. It is not possible to determine if this change in odor preference translates into an actual mating preference, because the females in which the SDN was masculinized were not exposed to the developmental androgens and estrogens required for masculinization of actual mating behavior, i.e., mounts and intromissions. Indeed, odor is not the sole influence on sex behavior or preference in rodents as well as other species.

An important caveat to the current results is that administration of minocycline or blocking antibodies to the lateral ventricles may have affected other sexually dimorphic brain regions relying on similar (as of yet, unknown) mechanisms involving microglial phagoptosis. The medial amygdala, BNSTp, and AVPV are sexually dimorphic nuclei that undergo extensive hormone-mediated cell death on a similar, albeit slightly earlier timeline to that observed in the SDN and are regions important for reproduction and social behavior (59). To date, none of the highly specific mechanisms establishing neuroanatomical sex differences in the brain have been found to generalize to other regions (29), but whether this is a universal rule is impossible to say. Future studies determining why certain cells are targeted for phagoptosis by microglia during a restricted developmental window and how this then determines adult behavior will provide further insights into the origins of sex differences in brain and behavior.

Materials and Methods

Rats. Adult Sprague–Dawley rats were purchased from Charles River Laboratories and bred in our facility on a 12:12-h reverse light cycle with ad libitum food and water. Pregnant dams were allowed to deliver naturally, and pups were designated post-natal zero (PN0) on the day of birth with litters culled to 14 pups per dam. Experiments were counterbalanced for sex and treatment across litters. All procedures were performed in accordance with the Institutional Animal Care and Use Committee's regulations at the University of Maryland School of Medicine.

Animal Treatments. Under cryoanesthesia, pups received bilateral intracerebroventricular (i.c.v.) infusions of 1 μL of mouse anti-CD11b (0.5 mg/mL; OX-42 clone, Bio-Rad) or mouse anti-F4/80 (Sigma-Aldrich; dose: 4 μg/2 μL total), minocycline hydrochloride (Sigma-Aldrich M9511; dose: 0.2 μg/2 μL total), or phosphate-buffered saline vehicle, over 60 s once per day on postnatal days 5 to 7 (or 5 to 8 for experiments that terminated on PN12 or 60 to 80) using a 23-gauge Hamilton syringe mounted to a stereotaxic manipulator placed 1 mm rostral to Bregma and 1 mm lateral from midline. Isolation of pups from the dam was kept to under 1 h.

Immunohistochemistry and Immunofluorescence. For neonatal endpoint analyses, postnatal day 8 rat pups were anesthetized with a lethal dose of Fatal Plus (Vortech Pharmaceuticals) and transcardially perfused with phosphate-buffered saline (PBS; 0.1M, pH 7.4) followed by 4% paraformaldehyde (PFA; 4% in PBS, pH 7.4). Brains were removed and post-fixed for 24 h in 4% PFA at 4 °C, then kept in 30% sucrose at 4 °C until fully submerged. Coronal sections were cut at a thickness of 45 μm on a cryostat (Leica CM2050S) and directly mounted onto silane-coated slides. For 3,3′-Diaminobenzidine (DAB) staining, slide-mounted sections were incubated in 0.01M sodium citrate (pH 6.0) for 20 min at 100 °C and allowed to cool to room temperature before being washed in Tris-buffered saline (TBS; 0.05M, pH 7.6). Slides were then incubated in 0.3% hydrogen peroxide in TBS for 30 min at room temperature. Sections were blocked with 5% bovine serum albumin (BSA) in TBS + 0.4% Triton X-100 (TBS-T). Sections were incubated overnight at room temperature with primary antibody containing 5% BSA in TBS-T. The next day, sections were washed in TBS, incubated in biotinylated secondary antibody for 1 h at room temperature followed by incubation in ABC reagent (1:500 dilution; Vectastain Elite ABC Kit, Vector Laboratories) in TBS-T for 1 h at room temperature, and visualized using DAB chromagen or nickel-enhanced DAB chromagen (0.05% 3,3′-diaminobenzidine, 0.2% nickel (II) sulfate, 0.006% hydrogen peroxide; Sigma-Aldrich). Sections were then counterstained with either cresyl violet or methyl green and coverslipped with DPX mounting medium. For fluorescent labeling, the immunohistochemistry procedure listed above was used for day 1, but on day 2, sections were incubated with fluorescent secondary antibody for 2 h at room temperature in the dark and coverslipped with ProLong Diamond Antifade (Thermo Fisher Scientific). Primary antibodies used and their dilutions are as follows: rabbit anti-Iba1 (Wako; 1:1,000), goat anti-Iba1 (Abcam; 1:1,000), rabbit anti-EGR1 (Cell Signaling Technologies; 1:500), rabbit anti-NeuN (Abcam; 1:2,000), rabbit anticleaved caspase 3 (Asp175) (Cell Signaling Technologies; 1:500), biotinylated goat antirabbit (Vector Laboratories; 1:500), biotinylated goat antimouse (Vector Laboratories; 1:500), Alexa Fluor 488 or 594 antirabbit, antigoat, antimouse (all made in donkey; Thermo Fisher Scientific; 1:500).

Image Acquisition and Analysis. For all experiments, confocal fluorescence images were acquired with either a Zeiss LSM 710 microscope equipped with 488, 561, and 633 lasers and 20× (1.0 NA) water-immersion and 100× (1.46 NA) oil immersion objective using Zeiss Zen software, or a Nikon A1 microscope equipped with 405, 488, 561, and 647 lasers and 20× (0.75 NA) and 100× (1.45 NA) oil-immersion objective and Nikon Elements software. Brightfield images were captured on a Nikon Eclipse E600 with a 4× or 20× objective and an MBF Bioscience CX9000 camera using Neurolucida software. Fluorescent images are displayed as maximum intensity projections of confocal z stacks (0.2 μm z step) using Imaris (Bitplane). For three-dimensional rendering of individual microglial cells, confocal z stacks were taken with a 100× objective, deconvolved using the automatic deconvolution algorithm in Nikon Elements, and reconstructed using Imaris (Bitplane). The Surfaces module was used to create a volumetric boundary of individual microglial cells, and the resulting microglial surface was used to mask subsequent channels to identify engulfed material. Each masked channel was then processed using the Surfaces module and merged with the microglial surface to create the final rendering.

Quantification of Phagocytic Microglia and SDN Size. Total and phagocytic microglia cell counts were performed using Neurolucida (MBF Bioscience). Microglia were considered for analysis if there was an observable cell body within the designated counting region and were considered to be phagocytic if the microglia contained at least one distinct phagocytic cup easily discernable from the cell body. The SDN was identified by Nissl density with either a cresyl violet or methyl green counterstain. Every section containing the SDN was used for analysis, and the SDN was traced in its entirety for a total of two to six sections per animal. Contours for the SDN and preoptic nuclei (medial, lateral, and central) were drawn using a 4× objective and preoptic nuclei were analyzed in the section containing the largest cross section of the SDN for both hemispheres. In a subset of samples, the cMPN of both hemispheres was analyzed in sections containing the first, middle, and last portions of the SDN.

Quantification of Phagocytic Cup Diameter and Contents. Fixed coronal sections were immunolabeled for Iba1 and either NeuN or cleaved caspase-3 and stained with DAPI, then imaged with a Nikon A1 confocal microscope. Single confocal images were taken with a 20× (0.75 NA) objective through the middle of the phagocytic cup. Images were then assessed for colocalization of NeuN/cleaved caspase 3/DAPI or measured for diameter using Nikon Elements software.

Quantification of Egr1+ Cells. Quantification of the number of Egr1+ cells across the SDN was performed using Neurolucida (MBF Bioscience). Contours outlining the boundaries of the SDN were drawn at 4× magnification and determined by Nissl density using a methyl green counterstain. Three sections randomly selected throughout the SDN were used to quantify the total number of Egr1+ cells for each animal using a 20× objective.

Quantification of SDN Cell Number. Quantification of the number of cell number within the SDN was performed using Neurolucida (MBF Bioscience). Contours outlining the boundaries of the SDN were drawn at 4× magnification and determined by Nissl density using a methyl green counterstain and all cells within the entire SDN counted using a 40× objective for sections generated at PN8 and a 20× objective for PN80. The sex and treatment condition of the animals were unknown to the investigator conducting the counts.

Behavioral Assessment.

Sexual odor preference. Animals were weaned on PN21 and housed in counterbalanced same sex, sibling groups of two to four. On PN60, animals were tested for 5 min in a three-chamber preference apparatus containing a central neutral zone flanked by two side choice chambers containing dishes of fresh soiled bedding from either a sexually active male or female in proestrus. The placement of odor cue was counterbalanced across treatment groups. A male preference score was calculated as follows: MPS = (time in male) − (time in female)/(time in male + time in female). Behavioral testing took place during the dark phase of the animal's light/dark cycle under red light illumination.

Sexual odor exposure for immediate early gene expression in cMPN. Between PN70-80, animals were isolated in their home cages for 1 h, after which they were exposed to filter paper soaked with urine from a sexually active stimulus male for 10 min. One hour later, animals were killed and brains harvested for immunohistochemical analysis of immediate early gene expression.

Statistical Analysis. All values are shown as the mean ± SEM. Statistical analysis was performed using GraphPad Prism (v9.4.0). Two-group comparisons were made using two-tailed Student's *t* test and multi-group by one-way or two-way ANOVA where appropriate with post hoc comparisons by Tukey's. Correlation coefficients were calculated by simple linear regression. A P value of <0.05 was used to determine significance.

Data, Materials, and Software Availability. Histological and behavioral quantification data have been deposited in Dryad (https://doi.org/10.5061/dryad.qbzkh18nj) (60).

ACKNOWLEDGMENTS. This work was supported by F31 NS093947 to L.A.P., F31 MH123025 to A.E.M., and R01 DA039062 and R01 MH52716 to M.M.M. The authors thank Dr. Troy Roepke and Dr. Jacques Balthazart for comments on an earlier draft of this manuscript.

1. R. A. Gorski, J. H. Gordon, J. E. Shryne, A. M. Southam, Evidence for a morphological sex difference within the medial preoptic area of the rat brain. *Brain Res.* **148**, 333–346 (1978).
2. F. Nottebohm, A. P. Arnold, Sexual dimorphism in vocal control areas of the songbird brain. *Science* **194**, 211–213 (1976).
3. C. Dulac, L. A. O'Connell, Z. Wu, Neural control of maternal and paternal behaviors. *Science* **345**, 765–770 (2014).
4. R. A. Gorski, R. E. Harlan, C. D. Jacobson, J. E. Shryne, A. M. Southam, Evidence for the existence of a sexually dimorphic nucleus in the preoptic area of the rat. *J. Comp. Neurol.* **193**, 529–539 (1980).
5. M. J. Sickel, M. M. McCarthy, Calbindin D28-K immunoreactivity is a marker for a subdivision of the sexual dimorphic nucleus of the preoptic area in the rat: Developmental profile and gonadal steroid modulation. *J. Neurobiol.* **12**, 397–402 (2000).
6. Y. Kato, S. Nakashima, F. Maekawa, S. Tsukahara, Involvement of postnatal apoptosis on sex difference in number of cells generated during late fetal period in the sexually dimorphic nucleus of the preoptic area in rats. *Neurosci. Lett.* **516**, 290–295 (2012).
7. C. E. Roselli, J. Balthazart, Sexual differentiation of sexual behavior and its orientation. *Front. Neuroendocrinol.* **32**, 109 (2011).
8. C. E. Roselli, K. Larkin, J. A. Resko, J. N. Stellflug, F. Stormshak, The volume of a sexually dimorphic nucleus in the ovine medial preoptic area/anterior hypothalamus varies with sexual partner preference. *Endocrinology* **145**, 478–483 (2004).
9. W. Byne *et al.*, The interstitial nuclei of the human anterior hypothalamus: An investigation of variation with sex, sexual orientation, and HIV status. *Horm. Behav.* **40**, 86–92 (2001).
10. S. LeVay, A difference in hypothalamic structure between heterosexual and homosexual men. *Science* **9**, 497–506 (1991).
11. E. A. Wilson, Neurological preference: LeVay's study of sexual orientation. *SubStance* **29**, 23–38 (2000).
12. M. McLaughlin, Is there a gay brain? The problems with scientific research of sexual orientation. *The Great Lakes J. Undergrad. Hist.* **6,** 45–60 (2018).
13. J. A. Morris, C. L. Jordan, S. M. Breedlove, Sexual differentiation of the vertebrate nervous system. *Nat. Neurosci.* **7**, 1034–1039 (2004).
14. N. M. Shah *et al.*, Visualizing sexual dimorphism in the brain. *Neuron* **43**, 313–319 (2004).
15. M. V. Wu, J. Tollkuhn, Estrogen receptor alpha is required in GABAergic, but not glutamatergic, neurons to masculinize behavior. *Horm. Behav.* **95**, 3–12 (2017).
16. M. V. Wu *et al.*, Estrogen masculinizes neural pathways and sex-specific behaviors. *Cell* **139**, 61–72 (2009).
17. R. W. Rhees, J. E. Shryne, R. A. Gorski, Onset of the hormone-sensitive perinatal period for sexual differentiation of the sexually dimorphic nucleus of the preoptic area in female rats. *J. Neurobiol.* **21**, 781–786 (1990).
18. C. D. Jacobson, R. A. Gorski, Neurogenesis of the sexually dimorphic nucleus of the preoptic area in the rat. *J. Comparat. Neurol.* **196**, 519–529 (1981).
19. C. D. Jacobson, F. C. Davis, R. A. Gorski, Formation of the sexually dimorphic nucleus of the preoptic area: Neuronal growth, migration and changes in cell number. *Brain Res.* **353**, 7–18 (1985).
20. R. W. Rhees, J. E. Shryne, R. A. Gorski, Termination of the hormone-sensitive period for differentiation of the sexually dimorphic nucleus of the preoptic area in male and female rats. *Dev. Brain Res.* **52**, 17–23 (1990).
21. E. C. Davis, P. Popper, R. A. Gorski, The role of apoptosis in sexual differentiation of the rat sexually dimorphic nucleus of the preoptic area. *Brain Res.* **734**, 10–18 (1996).
22. M. M. McCarthy, H. R. Besmer, S. C. Jacobs, G. M. O. Keiden, R. B. Gibbs, Influence of maternal grooming, sex and age on fos immunoreactivity in the preoptic area of neonatal rats: Implications for sexual differentiation. *Dev. Neurosci.* **19**, 488–496 (1997).
23. S. Tsukahara, M. Kakeyama, Y. Toyofuku, Sex differences in the level of Bcl-2 family proteins and caspase-3 activation in the sexually dimorphic nuclei of the preoptic area in postnatal rats. *J. Neurobiol.* **66**, 1411–1419 (2006).
24. S. Tsukahara, R. Hojo, Y. Kuroda, H. Fujimaki, Estrogen modulates Bcl-2 family protein expression in the sexually dimorphic nucleus of the preoptic area of postnatal rats. *Neurosci. Lett.* **432**, 58–63 (2008).
25. S. Tsukahara, Sex differences and the roles of sex steroids in apoptosis of sexually dimorphic nuclei of the preoptic area in postnatal rats. *J. Neuroendocrinol.* **21**, 370–376 (2009).
26. M. M. McCarthy, E. H. Schlenker, D. W. Pfaff, Enduring consequences of neonatal treatment with antisense oligodeoxynucleotides to estrogen receptor mRNA on sexual differentiation of rat brain. *Endocrinology* **133**, 433–439 (1993).
27. R. F. Gilmore, M. M. Varnum, N. G. Forger, Effects of blocking developmental cell death on sexually dimorphic calbindin cell groups in the preoptic area and bed nucleus of the stria terminalis. *Biol. Sex Differ.* **3**, 5 (2012).
28. N. G. Forger, Cell death and sexual differentiation of the nervous system. *Neuroscience* **138**, 929–938 (2006).
29. M. M. McCarthy, Multifaceted origins of sex differences in the brain. *Philos. Trans. R. Soc. Lond. B Biol. Sci.* **371**, 20150106 (2016).
30. M. M. McCarthy, L. A. Pickett, J. W. VanRyzin, K. E. Kight, Surprising origins of sex differences in the brain. *Horm. Behav.* **76**, 3–10 (2015), 10.1016/j.yhbeh.2015.04.013.
31. D. P. Schafer, E. K. Lehrman, B. Stevens, The "quad-partite" synapse: Microglia-synapse interactions in the developing and mature CNS. *Glia* **61**, 24–36 (2013).
32. D. P. Schafer *et al.*, Microglia sculpt postnatal neural circuits in an activity and complement-dependent manner. *Neuron* **74**, 691–705 (2012).
33. W. J. Streit, Microglial response to brain injury: A brief synopsis. *Toxicol. Pathol.* **28**, 28–30 (2000).
34. T. O. J. Cockram, J. M. Dundee, A. S. Popescu, G. C. Brown, The phagocytic code regulating phagocytosis of mammalian cells. *Front. Immunol.* **12**, 629979 (2021).
35. G. C. Brown, J. J. Neher, Eaten alive! Cell death by primary phagocytosis: "Phagoptosis." *Trends Biochem. Sci.* **37**, 325–332 (2012).
36. G. C. Brown, J. J. Neher, Microglial phagocytosis of live neurons. *Nat. Rev. Neurosci.* **15**, 209–216 (2014).
37. K. S. Ravichandran, Find-me and eat-me signals in apoptotic cell clearance: Progress and conundrums. *J. Exp. Med.* **207**, 1807–1817 (2010).
38. J. L. Marin-Teva *et al.*, Microglia promote the death of developing Purkinje cells. *Neuron* **41**, 535–547 (2004).
39. S. Wakselman *et al.*, Developmental neuronal death in hippocampus requires the microglial CD11b integrin and DAP12 immunoreceptor. *J. Neurosci.* **28**, 8138–8143 (2008).
40. F. Sedel, C. Bechade, S. Vyas, A. Triller, Macrophage-derived tumor necrosis factor alpha, an early developmental signal for motoneuron death. *J. Neurosci.* **24**, 2236–2246 (2004).
41. J. W. VanRyzin *et al.*, Microglial phagocytosis of newborn cells is induced by endocannabinoids and sculpts sex differences in juvenile rat social play. *Neuron* **102**, 435–449.e6 (2019), 10.1016/j.neuron.2019.02.006.
42. C. L. Cunningham, V. Martinez-Cerdeno, S. C. Noctor, Microglia regulate the number of neural precursor cells in the developing cerebral cortex. *J. Neurosci.* **33**, 4216–4233 (2013).
43. K. Elward, P. Gasque, "Eat me" and "don't eat me" signals govern the innate immune response and tissue repair in the CNS: Emphasis on the critical role of the complement system. *Mol. Immunol.* **40**, 85–94 (2003).
44. K. A. Jablonski *et al.*, Novel markers to delineate murine M1 and M2 macrophages. *PloS One* **10**, e0145342 (2015).
45. S. J. Kim *et al.*, Macrophages are the primary effector cells in IL-7-induced arthritis. *Cell Mol. Immunol.* **17**, 728–740 (2020).
46. S. Pierman, Q. Douhard, J. Balthazart, M. J. Baum, J. Bakker, Attraction thresholds and sex discrimination of urinary odorants in male and female aromatase knockout (ArKO) mice. *Horm. Behav.* **49**, 96–104 (2006).
47. S. Pierman, Q. Douhard, J. Bakker, Evidence for a role of early oestrogens in the central processing of sexually relevant olfactory cues in female mice. *Eur. J. Neurosci.* **27**, 423–431 (2008).
48. M. M. McCarthy, Estradiol and the developing brain. *Physiol. Rev.* **88**, 91–124 (2008).
49. G. W. Arendash, R. A. Gorski, Effects of discrete lesions of the sexually dimorphic nucleus of the preoptic area or other medial preoptic regions on the sexual behavior of male rats. *Brain Res. Bull.* **10**, 147–154 (1983).

50. R. B. Simerly, L. W. Swanson, R. J. Handa, R. A. Gorski, Influence of perinatal androgen on the sexually dimorphic distribution of tyrosine hydroxylase-immunoreactive cells and fibers in the anteroventral periventricular nucleus of the rat. *Neuroendocrinology* **40**, 501–510 (1985).
51. R. B. Simerly, L. W. Swanson, R. A. Gorski, Reversal of the sexually dimorphic distribution of serotonin-immunoreactive fibers in the medial preoptic nucleus by treatment with perinatal androgen. *Brain Res.* **340**, 91–98 (1985).
52. C. Orikasa, Y. Kondo, S. Usui, Y. Sakuma, Similar numbers of neurons are generated in the male and female rat preoptic area in utero. *Neurosci. Res.* **68**, 9–14 (2010).
53. M. Shayit, A. Weller, Cholecystokinin receptor antagonists increase the rat pup's preference toward maternal-odor and rug texture. *Dev. Psychobiol.* **38**, 164–173 (2001).
54. G. Gheusi, R. M. Bluthe, G. Goodall, R. Dantzer, Social and individual recognition in rodents: Methodological aspects and neurobiological bases. *Behav. Processes* **33**, 59–87 (1994).
55. C. D. Cisternas, L. R. Cortes, I. Golynker, A. Castillo-Ruiz, N. G. Forger, Neonatal inhibition of DNA methylation disrupts testosterone-dependent masculinization of neurochemical phenotype. *Endocrinology* **161**, bqz022 (2020).
56. S. Bhattacharya, R. Amodei, E. Vilain, C. E. Roselli, Identification of differential hypothalamic DNA methylation and gene expression associated with sexual partner preferences in rams. *PloS One* **17**, e0263319 (2022).
57. L. M. De Biase *et al.*, Local cues establish and maintain region-specific phenotypes of basal ganglia microglia. *Neuron* **95**, 341–356.e346 (2017).
58. E. I. Ahmed *et al.*, Pubertal hormones modulate the addition of new cells to sexually dimorphic brain regions. *Nat. Neurosci.* **11**, 995–997 (2008).
59. N. G. Forger, Control of cell number in the sexually dimorphic brain and spinal cord. *J. Neuroendocrinol.* **21**, 393–399 (2009).
60. Dryad, https://doi.org/10.5061/dryad.qbzkh18nj